



Assessing extracted organic matter quality from river sediments by elemental and molecular characterization: Application to the Tietê and Piracicaba Rivers (São

Carla Pereira de Moraes, Amanda Maria Tadini, Lucas Raimundo Bento, Benjamin Oursel, Francisco Eduardo Gontijo Guimaraes, Ladislau Martin-Neto, Stéphane Mounier, Débora Marcondes Bastos Pereira Milori

► To cite this version:

Carla Pereira de Moraes, Amanda Maria Tadini, Lucas Raimundo Bento, Benjamin Oursel, Francisco Eduardo Gontijo Guimaraes, et al.. Assessing extracted organic matter quality from river sediments by elemental and molecular characterization: Application to the Tietê and Piracicaba Rivers (São. Applied Geochemistry, 2021, 131, pp.105049. 10.1016/j.apgeochem.2021.105049 . hal-03289516

HAL Id: hal-03289516

<https://hal.science/hal-03289516>

Submitted on 17 Jul 2021

HAL is a multi-disciplinary open access archive for the deposit and dissemination of scientific research documents, whether they are published or not. The documents may come from teaching and research institutions in France or abroad, or from public or private research centers.

L'archive ouverte pluridisciplinaire **HAL**, est destinée au dépôt et à la diffusion de documents scientifiques de niveau recherche, publiés ou non, émanant des établissements d'enseignement et de recherche français ou étrangers, des laboratoires publics ou privés.

**Assessing extracted organic matter quality from river sediments by elemental and
molecular characterization: Application to the Tietê and Piracicaba Rivers (São
Paulo, Brazil)**

Carla Pereira de Morais^{1,2,3*}, Amanda Maria Tadini³, Lucas Raimundo Bento^{1,3},
Benjamin Oursel², Francisco Eduardo Gontijo Guimaraes⁴, Ladislau Martin-Neto³,
Stéphane Mounier^{2*}, Débora Marcondes Bastos Pereira Milori^{3*}

¹São Carlos Institute of Chemistry, University of São Paulo, 13566-590, São Carlos, SP,
Brazil.

²University of Toulon, Aix Marseille University, CNRS/INSU, IRD, MIO UM 110,
Mediterranean Institute of Oceanography, CS 60584 83041 – Toulon CEDEX 9,
France.

³Embrapa Instrumentation, 13560-970, São Carlos, SP, Brazil.

⁴São Carlos Institute of Physics, University of São Paulo, 13566-590, São Carlos, SP,
Brazil.

*Corresponding authors

Carla Pereira de Morais

E-mail: moraispcarla@gmail.com

Stéphane Mounier

E-mail: stephane.mounier@univ-tln.fr

Débora Marcondes Bastos Pereira Milori

E-mail: debora.milori@embrapa.br

27 **Abstract**

28 Urban river pollution causes serious problems to the environment, human health, and
29 water scarcity. Developing tools to identify and assess the health of aquatic river
30 systems is essential for monitoring the quality of rivers and implementing actions. This
31 study assesses the elemental and molecular characteristics of organic matter (OM)
32 extracted from river sediments and associates them with river quality. To assess the
33 quality of sediment cores, the most reactive and available OM from two urban rivers
34 (Tietê and Piracicaba Rivers, São Paulo, Brazil) was isolated with alkaline and water
35 solutions. It was then characterized by elemental composition, ultraviolet-visible
36 spectroscopy, and fluorescence excitation-emission matrix with parallel factor analysis.
37 The average yield of alkaline extraction was $40.71\% \pm 5.52\%$ of OM present in the bulk
38 sediments. Extracted organic matter from sediments (EOMSed) from the Tietê River
39 presented the highest average concentrations of non-purgeable organic carbon (NPOC)
40 and total organic nitrogen (TON), and the lowest average NPOC/TON molar ratios and
41 specific UV absorbance at 254 nm ($SUVA_{254}$). Considering the high degree of
42 eutrophication in the Tietê River, these results suggest a greater input of simple OM
43 with nitrogenous structures. The humic-like component in EOMSed was the most
44 abundant in both rivers. The aromaticity of EOMSed from the Piracicaba River was
45 evidenced by the greater contribution of complex structures in the form of aromatic and
46 polyaromatic moieties and higher $SUVA_{254}$. EOMSed from the Tietê River also featured
47 enhanced biological activity due to the greater contribution of microbial-derived
48 products and the presence of small molecules and nitrogenous structures. As this
49 combination of elemental and spectroscopic techniques successfully identified the

characteristics of extracted OM, it can be used as a tool to assess the global river quality.

Keywords: River sediments, Extracted organic matter, Fluorescence, Parallel factor analysis.

1. Introduction

Sediments consist of particle accumulation with different physical and chemical properties that are composed of inorganic and organic material. The particles are transported by water, air, erosion, and weathering processes and distributed along rivers (Murdoch and MacKnight, 1991; Schorer and Eisele, 1997). The sediments are biogeochemically active due to the presence of many microbes and the continuous input of organic and inorganic substances (He et al., 2019; Kumwimba et al., 2017).

Organic matter (OM) in the sediments can originate from external sources (allochthonous) or from the aquatic ecosystem itself (autochthonous) (Brailsford et al., 2019; Kindler et al., 2011). Moreover, rivers are responsible for transferring carbon (C) between the terrestrial biosphere and oceans, where this element is transformed and stored (Cole et al., 2007). In sediments, bacteria consume or decompose organic particles, thus reducing the mass of OM (Bloesch, 2009). The organic material resistant to microbial action and any remaining products are deposited on the bottom of rivers, along with terrestrial sediments (Burdige, 2007; Henrichs, 1992). OM is then remineralized, altered, or preserved during early diagenesis, which records input history (Engel and Macko, 2013).

The mobilization and quality of sediments are partially affected by anthropogenic actions that cause extensive changes in the aquatic environment (Bloesch, 2009). The excessive load of nutrients leads to the eutrophication of rivers,

which is a process of increasing the OM load in an aquatic ecosystem (Nixon, 1995). In areas with a high population density, the main sources of nutrients are domestic sewage discharge, industrial effluent, and water drained from agricultural areas (Kubo and Kanda, 2020; Smith et al., 2014). Sediments with high OM content promote oxygen consumption through decomposition, which can harm aquatic animals and plants (Duarte, 1995).

Barra Bonita Reservoir in São Paulo State, Brazil, is formed by the damming of the Tietê and Piracicaba Rivers, and it is the first of six reservoirs of the Middle Tietê River Basin (Rodrigues et al., 2020). The Tietê and Piracicaba basins have different water resource management strategies, with different types of land use and occupation (Cruz et al., 2017). Both rivers receive a high degree of organic compounds, although the Tietê River is more eutrophic than the Piracicaba River, because it receives a large load of industrial and domestic waste (dos Santos et al., 2006; Morais et al., 2021; Rodrigues et al., 2020). The Middle Tietê River had a biochemical oxygen demand (BOD) of 33,636 t day⁻¹ in 2017 (CETESB, 2018). Before reaching the reservoir, the Tietê River passes through the metropolitan area of São Paulo (Upper Tietê River), which has a high population density and presented a BOD of 612,069 t day⁻¹. This represents 57% of BOD of the Tietê River. By comparison, the Piracicaba Basin had a BOD of 94,818 t day⁻¹ (CETESB, 2018). According to the State of São Paulo Environmental Company (CETESB), the courses of both aquatic bodies are situated in industrial areas marked by a high demographic density and intense land use (CETESB, 2018). However, regarding the course of the Middle Tietê River, its non-compliance with water-quality standards stands at around 100% due to the untreated sewage discharge in this stretch of the Tietê River (CETESB, 2018).

99 In the current scenario of scarce freshwater resources in terms of both the quality
100 and quantity available for use, it is urgent to restore water bodies. One way to do so is to
101 focus on assessing OM quality in sediments. Furthermore, finding the tools to identify
102 and assess the health of aquatic river systems is essential for the implementation of
103 actions. Molar C to nitrogen (N) ratios can be useful to identify the origin of OM
104 (Burone et al., 2003; Meyers, 1994), whereas determining the optical properties of OM
105 present in sediments is also a rapid and efficient way to assess the quality of water
106 resources and obtain information about anthropogenic activities (Du et al., 2021). OM is
107 a small fraction of the sediment compared to the inorganic fraction. The extraction is
108 carried out to isolate part of the OM and obtain information about its origin and quality.
109 For this purpose, water or basic extractants have shown their potential for determining
110 the quality and origin of OM in sediments (Brym et al., 2014; Funkey et al., 2019). The
111 neutral aqueous medium allows for the extraction of polar substances of small
112 molecular weight, which are free from the mineral fraction in the sediments. Water
113 alkaline extraction favors the extraction of more polar or reactive substances, even
114 allowing for the extraction of substances linked to minerals (Olk et al., 2019). After the
115 extraction with neutral and basic water, there remains only an insoluble organic fraction
116 that is strongly linked to minerals. This can be considered a stable or less reactive OM,
117 which will hardly influence the chemical processes in the sediment (Guigue et al., 2014;
118 Muller et al., 2014; Olk et al., 2019).

119 To assess the sediment quality, the most available and reactive OM was isolated
120 with neutral and alkaline water solutions. It was then fully characterized by elemental
121 composition, ultraviolet-visible spectroscopy (UV-Vis), and fluorescence excitation-
122 emission matrix (EEM) processed with parallel factor analysis (PARAFAC). This study
123 aimed to evaluate the elemental and molecular features of the extractable OM of

sediments taken from the Piracicaba and Tietê Rivers and associate this information with the global river quality.

2. Materials and methods

2.1. Study area description and sediment sampling

The study area covers the Tietê and Piracicaba Rivers upstream from the Barra Bonita Reservoir. The Barra Bonita Reservoir, located between the cities of Barra Bonita and Igarapu do Tietê, was created from the flooding and damming of these rivers (Bernardo et al., 2016). The Tietê and Piracicaba Rivers pass through large urban centers until their confluence. Both rivers receive a large load of organic and inorganic pollutants, which are delivered to the reservoir, although a greater load of pollutants is dumped into the Tietê River (Smith et al., 2014). The study area was chosen due to the different uses and occupations of the soil in this region, characterized by pollution issues and multiple uses of water. Furthermore, this region has suffered from many anthropic actions, mainly due to deforestation and flooding for the construction of six successive reservoirs, with the Barra Bonita Reservoir being the first (Rodrigues et al., 2020).

The sediment cores were collected at seven points: three on the Piracicaba River (stations 1, 2, and 3), one at the confluence region (station 4), and three on the Tietê River (stations 5, 6, and 7) (Figure 1) (Moraes et al., 2021). The collection points were georeferenced using a GPS Trimble Navigation unit as shown in the supplementary material (Table S1); the sampling took place on July 25, 2017 (austral winter). The sediment samples were collected using core sampling, which allowed us to maintain the original deposition of sedimentary layers. The horizontal slicing was performed at the same time as the sample collection, in different sizes (Table S2) under normal

atmosphere along the sediment cores without removing the interstitial water, thus totaling 69 sample layers. The sediment samples were immediately packed into polypropylene flasks and kept in a thermal box during transport to the laboratory to avoid the oxidation effect.

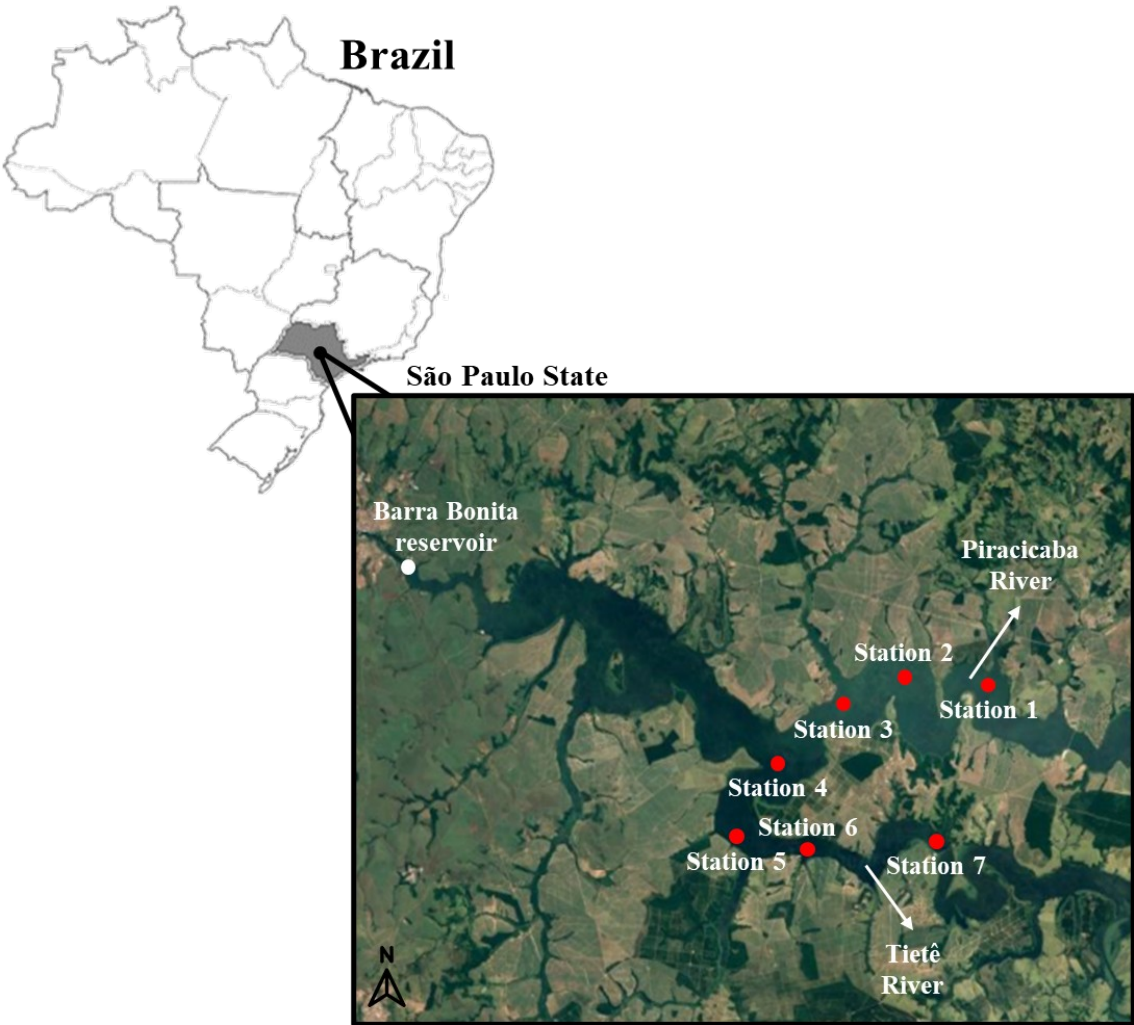


Figure 1: Location of the Barra Bonita Reservoir (white dot) and sediment sample collection stations (red dots).

2.2. Elemental analysis

The sediment samples were frozen, freeze-dried (L101, Liotop), crushed using an automatic mortar grinder (RM 200, Retsch), and sieved through a 100-mesh sieve. Total carbon (TC) content of the sediment samples was assessed using the dry

combustion method. For this purpose, 20 mg of the homogenized samples were accurately weighed directly in the tin capsules. The standard used in the analysis was aspartic acid, and the method was validated using the soil certified reference material (ThermoFisher Soil Reference Material NC PN338 40025). All measurements were performed in an elemental analyzer (Flash 2000, ThermoFisher Scientific).

2.3. Extractable organic matter from sediment samples

2.3.1. Extraction

The alkaline extraction was performed with NaOH to isolate OM in the sediment samples taken from the Piracicaba and Tietê Rivers. The sediment extracts were denominated EOMSed (extracted organic matter from sediments). Approximately 1.0 g of each sample was placed in polypropylene flasks with 45.0 mL of 0.1 mol L⁻¹ NaOH (ThermoFisher Scientific) and shaken for 24 h in an overhead shaker (Rex 20, Heidolph) at 10 rpm. The samples were then centrifuged (Sigma 3-18K, Grosseron) at 10,000 rpm for 10 min and filtered over 0.45 µm syringe filters (Minisart NML, Sartorius). Furthermore, another extraction method was conducted in the same way as previously described with 45.0 mL ultrapure water (Ultrapure Water Cell, Starna Ltd) in which the extracts from sediments were denominated WEOMSed (water-extracted organic matter from sediments).

2.3.2. Non-purgeable organic carbon and total organic nitrogen determination

Non-purgeable organic carbon (NPOC) and total organic nitrogen (TON) from EOMSed were quantified after dilution with ultrapure water to fit the standard NPOC calibration curve (maximum 30 mg L⁻¹ of C). The extracts were acidified and measured using an elemental analyzer (TOC-V Shimadzu). The NPOC/TON molar ratios were

calculated. The extraction yield was obtained by dividing the quantity of organic carbon (OC) in the extracted solution in mg (NPOC multiplied by the extraction volume) by the carbon content in the corresponding sediment in mg (TC multiplied by extracted mass sample).

2.3.3. *UV-Vis spectroscopy*

Absorbance measurements were performed for all EOMSed and WEOMSed samples using a double beam UV-Vis spectrophotometer (UV 1800, Shimadzu) with a wavelength range from 200 to 700 nm in a 1 cm path length quartz cell and a scan speed of 300 nm min⁻¹. A reference cell of NaOH and deionized water was used to measure EOMSed and WEOMSed, respectively. From the absorbance measurements, it was possible to define the dilution factor for fluorescence. Thus, all samples had the absorbance adjusted to 0.1 at 254 nm, thus allowing their comparisons by avoiding the inner filter effect for the fluorescence analysis (Kothawala et al., 2013). Specific UV absorbance at 254 nm (SUVA₂₅₄) was calculated by dividing the UV absorbance measured at 254 nm by the NPOC concentration (mg of C L⁻¹) and the optical path of the cuvette (0.01 m) (Weishaar et al., 2003).

2.3.4. *Fluorescence spectroscopy*

2.3.4.1. *Sample preparation and analysis*

For the study of EEM, 1.0 mL of each sample diluted to absorbance at 254 nm equal 0.1 (1 cm path length) was placed in quartz cells along with 1.0 mL of 0.3 mol L⁻¹ HEPES (Acros Organics) for pH regulation at 7 and 1.5 mL of 0.1 mol L⁻¹ NaClO₄ (Sigma-Aldrich) with a purity of 99.99% to fix ionic strength. The samples were analyzed immediately after preparation.

All measured spectra were obtained with a fluorescence spectrofluorometer (F4500, Hitachi). The EEM spectra were acquired with an excitation range from 200 to 500 nm and an emission range from 250 to 700 nm at a scan speed of 2400 nm min⁻¹. The steps and slits of emission and excitation were fixed at 5 nm, and the detector voltage was 700 V. Both emission and excitation detectors were corrected to prevent wavelength sensitivity. The Raman spectrum of ultrapure water (Ultrapure Water Cell, Starna Ltd) was measured on a daily basis with excitation at 350 nm, scan speed at 240 nm min⁻¹, emission from 360 to 420 nm, and excitation and emission slit fixed at 5 nm and 700 V to normalize the EEM intensity with the Raman scattering peak (Lawaetz and Stedmon, 2009).

2.3.4.2. Fluorescence data processing

PARAFAC was conducted on the EEM dataset using PROGMEEF software (<https://woms18.univ-tln.fr/progmeeef/>) in Matlab language. All the EEMs were cleaned from the diffusion signals using Rayleigh scattering by cutting the diffusion band in 15 nm and using first- and second-order Raman scattering by applying the Zepp method (Mounier et al., 2011; Zepp et al., 2004). The number of evaluated components varied from 2 to 5 in a spectral range from 240 to 500 nm in excitation and from 250 to 700 nm in emission. The number of components was defined using the core consistency diagnostic (CORCONDIA). The optimal rank was the model giving the higher number of components with a CORCONDIA over 60% (Mounier et al., 2011). The excitation and emission of components obtained by PARAFAC were compared to the OpenFluor database (Murphy et al., 2014).

2.4. Statistical analysis

Unpaired t-tests were used to determine any statistical differences between the TC in bulk sediments from the Tietê and Piracicaba Rivers and NPOC, TON, NPOC/TON molar ratios, and SUVA values obtained for EOM_{Sed} from the Tietê and Piracicaba Rivers. The correlation coefficient between the NPOC/TON molar ratios and the SUVA₂₅₄ values was calculated.

3. Results and discussion

3.1. Total carbon characteristics in bulk sediments

The distributions of TC content in the bulk sediment cores in the Piracicaba and Tietê Rivers were different (Figure 2). In the collection stations of the Piracicaba River (stations 1, 2, and 3), the highest TC value was found in the upper layer of the sediment cores, and a decrease in TC content was observed at the lower layers of the vertical distribution. In station 1, TC varied from 1.96% to 2.60% with a coefficient of variation (CV) of 0.10, and the lowest value at a depth of 41 cm. In station 2, TC varied from 2.12% to 3.32% (CV = 0.15), and despite the decrease in TC when entering the sediment, it was possible to observe an increase in TC content between the depths of 30 cm and 32 cm. In station 3, TC varied from 2.24% to 4.94% (CV = 0.30), although it decreased exponentially from the surface to a depth of 27.5 cm, and from that depth, it remained almost constant. In the confluence region, TC varied from 2.44% to 5.76% (CV = 0.27), although the highest TC content is found in the surface layer, as in the collection stations of the Piracicaba River. Its behavior is more similar to the collection stations located on the Tietê River, which present a random TC distribution in the deeper layers of the sediment cores. TC variation in the Tietê River ranged from 3.09% to 6.59% (CV = 0.19), 1.44% to 3.66% (CV = 0.26), and 3.25% to 5.77% (CV = 0.19) at stations 5, 6, and 7, respectively.

261 TC content is a fundamental parameter to describe the abundance of OM and
262 inorganic carbon (IC) in sediments (Veres, 2002). The random distribution of TC in the
263 Tietê River may be associated with an irregular input of OM and IC. A unpaired t-test
264 with a 95% confidence level showed that there were significant differences between the
265 average TC of the rivers. The average TC content in the Tietê River (3.96 ± 1.11) is
266 higher than in the Piracicaba River (2.57 ± 0.58). The highest TC content for the Tietê
267 River suggests that this river is more eutrophic than the Piracicaba River, since the
268 accumulation of nutrients, mainly P and N, in the aquatic bodies increases the synthesis
269 of OM (Castillo, 2020). This hypothesis is corroborated by a study that we previously
270 published on the quantification of total phosphorus (TP) in the same sediment samples
271 studied here (Morais et al., 2021). As TP is a chemical variable used to assess the
272 nutrient load and the extent of eutrophication in water bodies, the higher average TP
273 content in the Tietê River ($4316.16 \pm 1062 \text{ mg kg}^{-1} \text{ P}$) than in the Piracicaba River
274 ($1800.17 \pm 696.82 \text{ mg kg}^{-1} \text{ P}$) indicates that this river has a higher degree of
275 eutrophication (Morais et al., 2021).

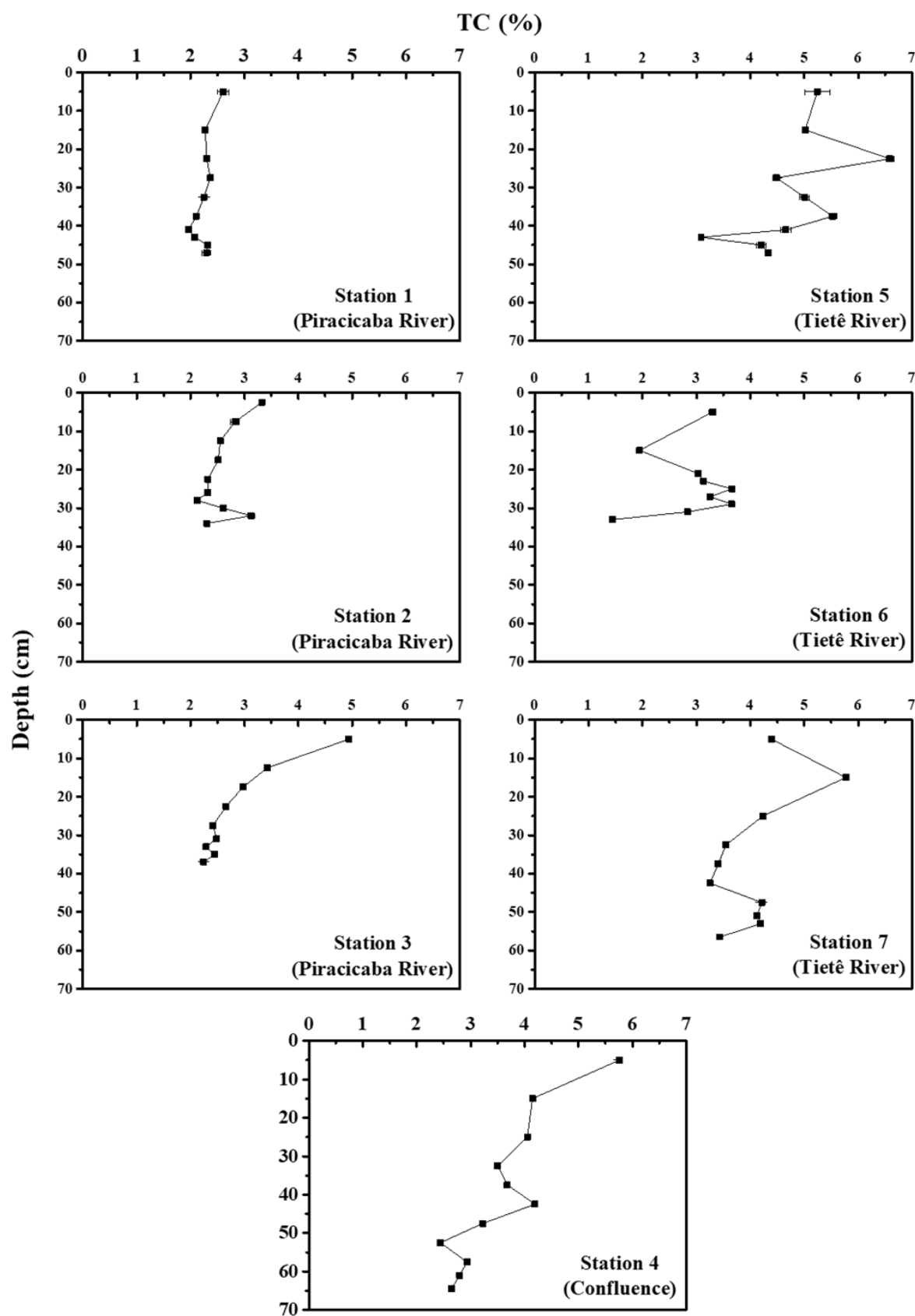


Figure 2. Total carbon distribution inside the sediment cores at the collection stations.

3.2. Characteristics of extracted organic matter from sediments

Table 1 shows the average concentration of NPOC and TON, alkaline extraction yield, NPOC/TON molar ratio, and SUVA₂₅₄ of EOMSed at the different stations. These values for each sample are shown in the supplementary material (Table S3). The extraction method with alkaline solution extracted an average of 40.71% ± 5.52% of OM present in the bulk sediments. The yield of OM extraction depends on the property of the extractant and is generally low. Among the different extractants used for OM extraction, NaOH seems to be the most effective (Kurek et al., 2020; Sire et al., 2009).

Table 1. Average concentration of non-purgeable organic carbon (NPOC) and total organic nitrogen (TON), alkaline extraction yield, NPOC/TON molar ratio, and specific UV absorbance at 254 nm (SUVA₂₅₄) of the extracted organic matter from sediments at the collection stations.

Station	NPOC (mg C g ⁻¹)	TON (mg N g ⁻¹)	Extraction yield (%)	NPOC/TON ratio	SUVA ₂₅₄ (L mg ⁻¹ m ⁻¹)
1	9.02±0.84	1.14±0.11	40.63±5.17	6.80±0.20	6.36±0.53
2	10.65±1.71	1.25±0.24	41.03±3.58	7.37±1.00	5.99±0.69
3	12.59±1.98	1.75±0.38	45.23±6.56	6.22±0.49	6.11±1.08
4	13.54±4.82	2.40±0.76	37.17±5.61	4.78±0.30	4.54±0.73
5	19.60±5.74	3.01±0.74	40.11±5.17	5.53±0.50	3.92±0.61
6	11.90±3.54	2.00±0.52	40.50±3.96	5.05±0.37	3.70±0.51
7	16.24±2.31	2.51±0.45	41.05±6.36	5.59±0.32	4.44±0.83

292

293 A unpaired t-test at the 95% confidence level demonstrated that there were
294 significant differences in the NPOC and TON averages of EOMSed in the Tietê and
295 Piracicaba Rivers. The average concentration of NPOC and TON of EOMSed in the
296 Tietê River ($16.05 \pm 5.10 \text{ mg C g}^{-1}$ and $2.52 \pm 0.70 \text{ mg N g}^{-1}$, respectively) was higher
297 than that in the Piracicaba River ($10.69 \pm 2.11 \text{ mg C g}^{-1}$ and $1.37 \pm 0.37 \text{ mg N g}^{-1}$,
298 respectively). The highest NPOC concentrations of EOMSed in the Tietê River may be
299 due to the fact that the river passes through the metropolitan area of São Paulo, where it
300 receives a large load of domestic sewage and industrial effluents, resulting in a larger
301 biological oxygen demand than the Piracicaba River (CETESB, 2018). Furthermore,
302 taking into account the history of the Tietê River, its high degree of contamination
303 (Rocha et al., 2011, 2010) and eutrophication (Morais et al., 2021), the higher TON
304 concentration of EOMSed in the Tietê River when compared to the Piracicaba River
305 may be due to the sewage discharge containing labile and fresh OM.

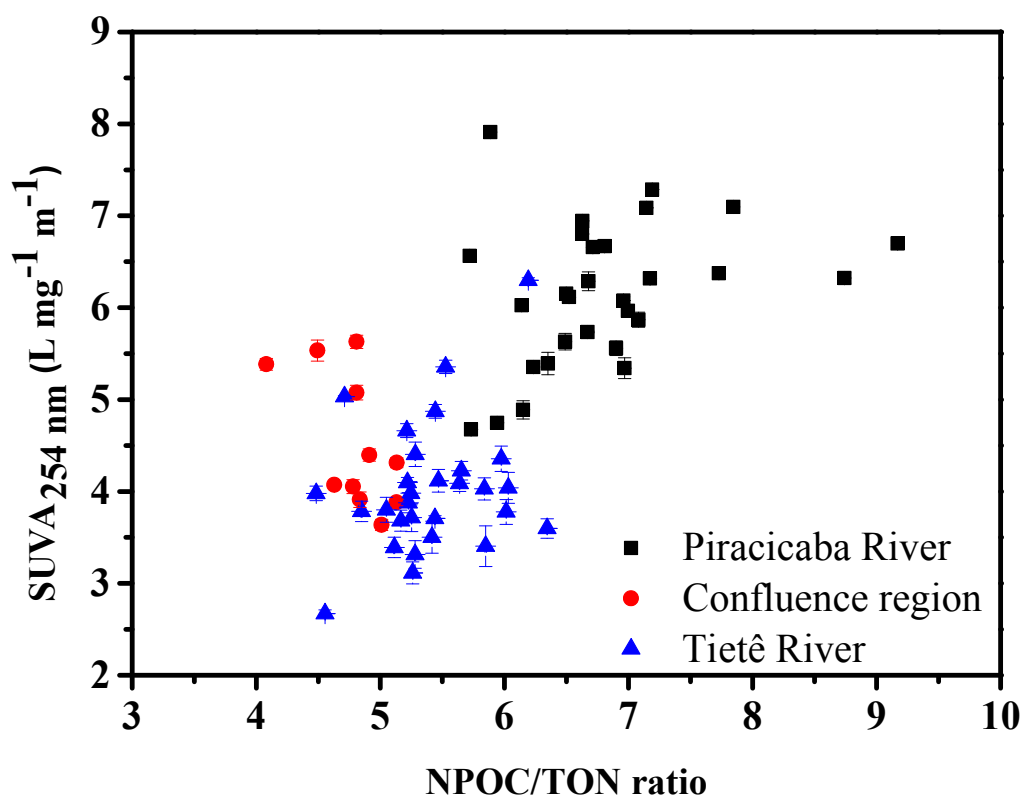
306 The average NPOC/TON molar ratios of EOMSed in the Tietê and Piracicaba
307 Rivers were statistically different (95% confidence level, unpaired t-test) and were
308 higher for the Piracicaba River (6.80 ± 0.79) compared to the Tietê River (5.39 ± 0.46).
309 Considering the historical course of the Tietê River and its high degree of
310 eutrophication (Morais et al., 2021), the lower ratios found in the river may suggest a
311 larger input of simple OM with nitrogenous structures, which may indicate effluent
312 input. In the confluence region, the NPOC/TON molar ratio of EOMSed was the lowest:
313 4.78 ± 0.30 . The lower value of the NPOC/TON molar ratio shows an increase in OM
314 deposition with nitrogenous structures, suggesting that the confluence region is
315 predominantly influenced by the Tietê River, which showed the highest nitrogen

316 concentrations (range of 2.00–3.01 mg N g⁻¹). Despite the difference in the NPOC/TON
317 molar ratios of EOM_{Sed} between the Tietê and Piracicaba Rivers, the studied EOM_{Sed}
318 showed a NPOC/TON molar ratio that varied from 4.1 to 9.2 (Figure 3). The
319 NPOC/TON molar ratios between 4 and 10 categorize the sources of C and N of algae
320 and aquatic plants (Kaushal and Binford, 1999; Meyers, 1994).

321 SUVA₂₅₄ is associated with the aromaticity of OM due to the carbon double
322 bond (C=C) of aromatic moieties or polycondensated aromatic rings that absorb light at
323 254 nm (Edzwald and Tobiasson, 2011). Therefore, high SUVA₂₅₄ values indicate an
324 OM formed by more structures that absorb light at 254 nm per unit concentration of OC
325 (Edzwald and Tobiasson, 2011). The average SUVA₂₅₄ values of EOM_{Sed} in the
326 Piracicaba and Tietê Rivers were statistically different (95% confidence level, unpaired
327 t-test) and were higher for the Piracicaba River (6.16 ± 0.78) than the Tietê River (4.02
328 ± 0.71). The confluence region showed SUVA₂₅₄ values of EOM_{Sed} closer to the Tietê
329 River (average SUVA₂₅₄ values was 4.54 ± 0.71 L mg⁻¹ m⁻¹). SUVA₂₅₄ showed
330 differences in the composition of EOM_{Sed} between the two rivers, with the higher
331 average SUVA₂₅₄ values for the Piracicaba River indicating that EOM_{Sed} has a
332 relatively high aromatic content compared to the Tietê River.

333 The NPOC/TON molar ratios of EOM_{Sed} were correlated with the SUVA₂₅₄
334 values (Figure 3). Regression analysis found a positive relationship between the
335 NPOC/TON molar ratio and SUVA₂₅₄ ($r = 0.67$; $p < 0.001$). By analogy to soil OM,
336 these results could be associated with the functional complexity of EOM_{Sed} (Dungait et
337 al., 2012; Lehmann et al., 2020). During the degradation of OM, the more polar
338 structures are more accessible to microorganisms and are thus consumed faster,
339 resulting in an accumulation of OM that is thermodynamically unfavorable to
340 microorganisms (hydrophobic and aromatic moieties). The relatively lower presence of

341 N suggests that these structures have already been totally or partly assimilated, resulting
 342 in the selective preservation and accumulation of more chemically stable structures,
 343 which led to greater aromaticity in the Piracicaba River. Conversely, the lower $SUVA_{254}$
 344 and NPOC/TON molar ratio in the Tietê River suggest the addition of fresh OM. This
 345 evidence is supported by the high BOD value of the Tietê River.



346
 347 **Figure 3.** Relationship between specific UV absorbance at 254 nm ($SUVA_{254}$) and non-
 348 purgeable organic carbon (NPOC) and total organic nitrogen (TON) molar ratios of
 349 extracted organic matter from sediments.

350

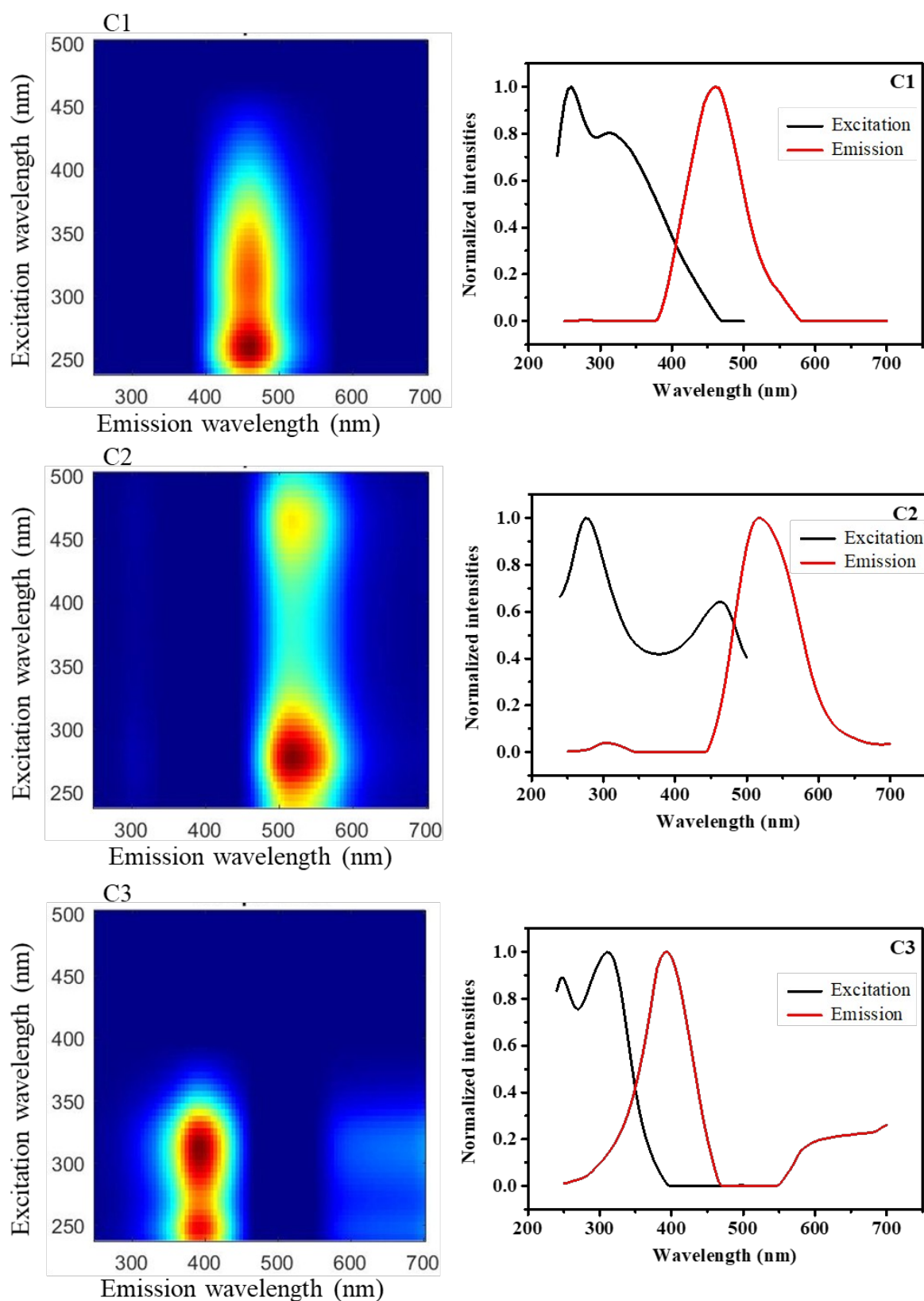
351 3.3. Fluorescence excitation-emission matrix spectra of organic matter extracted from 352 sediments with alkaline and neutral water solutions

353 The PARAFAC model adjusted for EEM (N= 138) from EOMSed and
 354 WEOMSed diluted to the same optical density resulted in three fluorescent components
 355 (Figure 4) with a CORCONDIA of 89.98%. The spectral characteristics of the three

356 components were compared to the OpenFluor database (Murphy et al., 2014), and
357 similarity was measured with the PARAFAC models from different aquatic
358 environments using the EEM similarity score of 0.95. Components 1, 2, and 3
359 respectively corresponded to PARAFAC models 35, 5, and 25 from the OpenFluor
360 database.

361 Component 1 (C1) had two excitation maxima: one in 260 nm stimulated by UV
362 excitation (peak A), and the other in 310 nm stimulated by visible excitation, with an
363 emission maximum in the visible range at 465 nm for both excitation peaks (Coble,
364 1996). Component 2 (C2) was comprised of two excitation maxima at 285 nm and 465
365 nm, and an emission maximum at 520 nm (Osburn et al., 2011; Walker et al., 2013).
366 The fluorescence emission is useful to access the structural arrangement of OM due to
367 the fluorophore emission in short (blue-shift) or long wavelength (red-shift). C1 and C2
368 had similar characteristics to soil fulvic and humic acids, respectively. C1 resembles
369 fulvic acids due to the shorter wavelength emission, and the blue-shifted component is
370 attributed to the lower molecular weight and a structural arrangement comprised of
371 more alkyl moieties (Borisover et al., 2009; Kowalczyk et al., 2009; Osburn et al., 2016,
372 2011; Shutova et al., 2014; Yamashita et al., 2010b, 2010a). C2 resembles humic acids
373 from the soil due to the red-shifted component, which is attributed to a more complex
374 structural arrangement mainly composed of aromatic moieties (Soares da Silva et al.,
375 2020). Furthermore, the shift in the wavelength concerns the aggregation of humic
376 structures in solution; a red-shifted humic structure can show a molecular arrangement
377 with higher molecular aggregation, while a shorter wavelength suggests smaller
378 molecules (Bento et al., 2020; Boguta and Sokołowska, 2020, 2016). Component 3 (C3)
379 demonstrated two excitation maxima at 250 nm and 315 nm, and an emission maximum
380 at 395 nm. C3 resembled microbial humic-like compounds from aquatic environments

381 (Coble, 1996; Osburn et al., 2011). This component is probably a product of microbial
 382 activity and thus of autochthonous origin (Yamashita et al., 2008).



383

Figure 4. Excitation-emission matrix contour plots of the three parallel factor analysis components (left) and their excitation and emission spectra (right).

The PARAFAC model was made for a dataset with all samples, thus allowing us to compare the component contributions. Figures 5 and 6 show the fluorescent contributions of each component identified by PARAFAC for EOMSed and WEOMSed, respectively, along with the sediment cores in the different stations, corrected for the analytical dilution factor. For EOMSed (Figure 5), the average fluorescent contribution of C1 was higher in decreasing order for the Piracicaba River > Tietê River > confluence region. This shows that small molecules make a greater contribution to the EOMSed arrangement of the Piracicaba River. The average fluorescent contribution of C2 had the same decreasing order as that of C1 (Piracicaba River > Tietê River > confluence region), showing that complex structures in the form of aromatic and polyaromatic moieties make a greater contribution to the EOMSed arrangement of the Piracicaba River. The average fluorescent contribution of C3 was higher in decreasing order for the Tietê River > Piracicaba River > confluence region, showing that microbial-derived products make a greater contribution to the EOMSed arrangement of the Tietê River. Thus, EOMSed from the Piracicaba River contains more aromatics, while EOMSed from the Tietê River contains more microbial-derived products. These results are in agreement with the $SUVA_{254}$ values and NPOC/TON molar ratios, which showed less aromatic EOMSed with more nitrogenous structures for the Tietê River compared to the Piracicaba River. The low NPOC/TON molar ratio may be the main reason for the higher microbial activity and the consequent presence of microbial derivatives (C3).

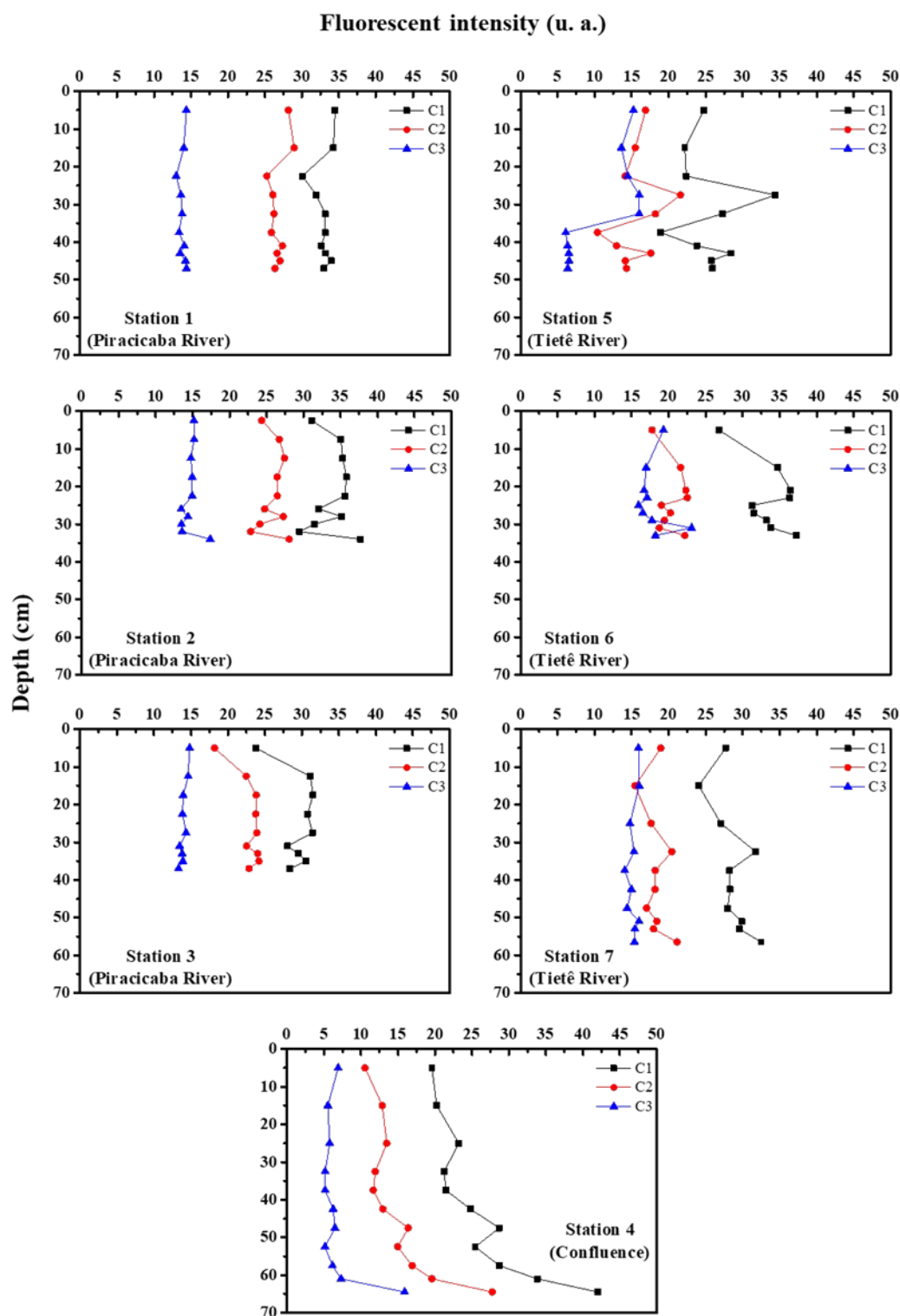


Figure 5. Fluorescent intensity of components (C1, C2, and C3) taken from the extracted organic matter from sediments along with the sediment core identified by parallel factor analysis.

In WEOM_{Sed} (Figure 6), the average fluorescent contributions of C1, C2, and C3 were higher in decreasing order for the confluence region > Tietê River > Piracicaba River. The extraction of microbial-derived products (C3) was greater for WEOM_{Sed} than for EOM_{Sed}, and the C3 values were higher at the stations of the Tietê River than the Piracicaba River, indicating its greater microbial activity. The low abundance of C2 can be ascribed to the component structure, because humic-like substances with high aromaticity are more soluble in alkaline solution than in water, which may result in the higher relative content of C2 in alkaline solution; furthermore, the higher C2 concentration in alkaline extracts obfuscates the C3 concentration. The alkaline medium favored the greater extraction of C1 and C2 (humic-like compounds) due to the hydrolysis caused in the functional groups of humic molecules bonded to the surface of the mineral from sediment (Kleber and Lehmann, 2019; Olk et al., 2019).

The optical properties of EOM_{Sed} proved to be more efficient for assessing the quality and composition of sediments than those of WEOM_{Sed} due to the better discrimination between the fluorescence components in the alkaline extracts. Although water extraction has been used to assess OM sources and link contamination in polluted urban rivers (Chen et al., 2019; Zhang et al., 2020), in our study, alkaline extracts were better at describing the properties of OM.

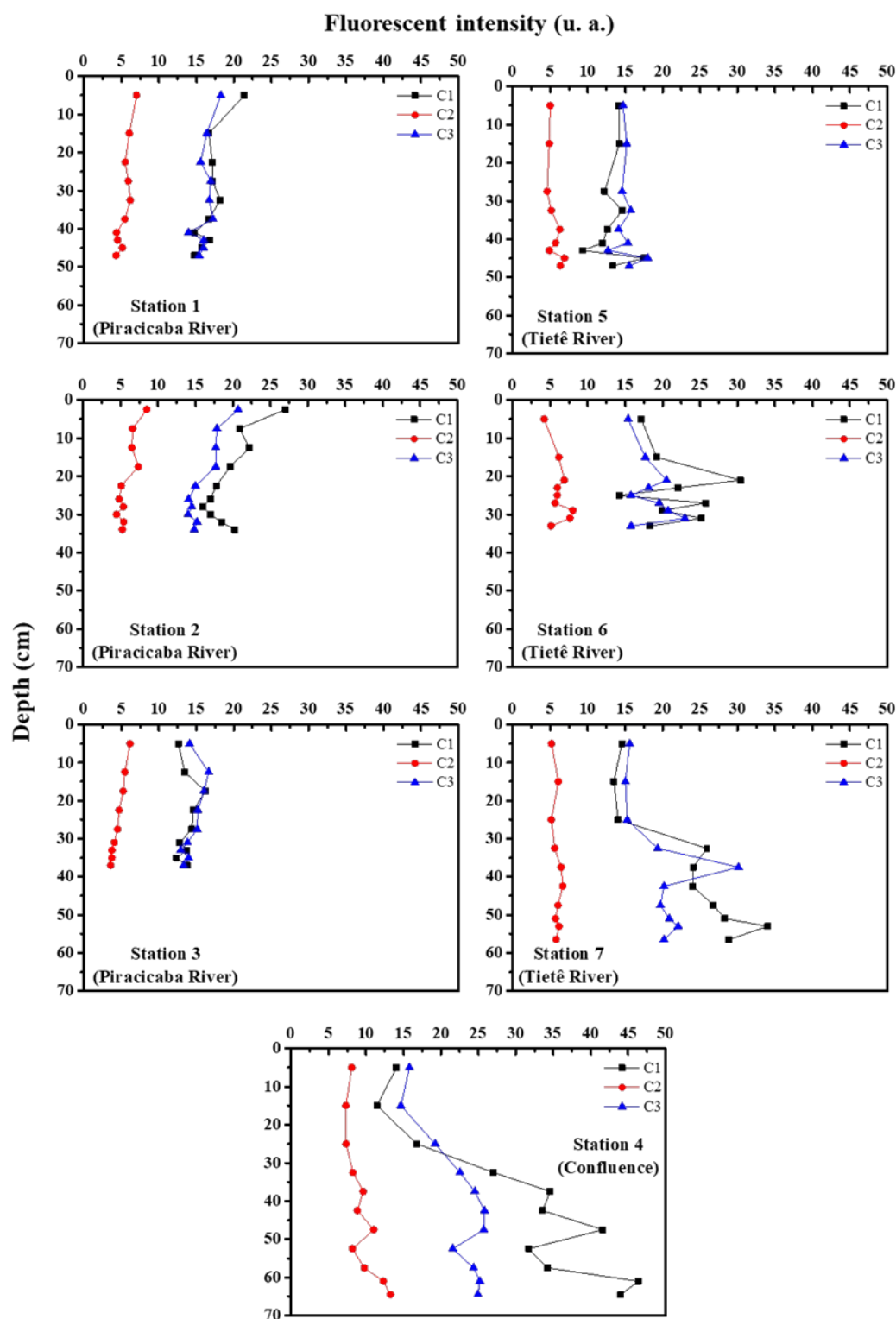


Figure 6. Fluorescent intensity of components (C1, C2, and C3) taken from water-extracted organic matter from sediments along with sediment core identified by parallel factor analysis.

3.4. Features of extractable organic matter from sediments from the Piracicaba and Tietê Rivers

The neutral water solution enabled the better extraction of small molecules (blue-shifted), which are free from the mineral fraction in the sediments. While the alkaline solution favors the extraction of more complex substances (red-shifted). The results obtained with EEM-PARAFAC together with $SUVA_{254}$ values and NPOC/TON molar ratio allowed for the total assessment of EOMSed quality.

The differences between the EOMSed compositions in sediments were highlighted by the $SUVA_{254}$ values, NPOC/TON molar ratios, and EEM-PARAFAC. Although the most abundant component in EOMSed from the two rivers is humic-like with the lowest molecular weight (C1), the aromaticity of EOMSed from the Piracicaba River was evidenced by the greater contribution of C2 and $SUVA_{254}$ values. Conversely, EOMSed from the Tietê River had greater microbial activity due to the greater contribution of C3, the presence of small molecules (lower C2 contribution), and the presence of nitrogenous structures. Based on the analyses performed, it was not possible to further identify the compositional alteration of EOMSed and WEOMSed, which may be related to their similar deposition.

The origin of EOMSed is inferred from the results obtained here. The NPOC/TON molar ratios calculated for EOMSed from the Piracicaba River indicate that EOMSed can form in the aquatic body (autochthonous). The contributions of two humic-like components in alkaline extracts indicate that EOMSed may also originate from soil OM (allochthon). According to the NPOC/TON molar ratios calculated for EOMSed from the Tietê River as well as the greater microbial activity in this aquatic ecosystem, it can be inferred that the origin of EOMSed is predominantly

allochthonous, mainly due to the discharge of domestic sewage, which is indicated by the higher content of TC present in the Tietê River sediments.

4. Conclusion

EOM_{Sed} from the Piracicaba and Tietê Rivers was mainly characterized by an arrangement of low molecular weight compounds. However, EOM_{Sed} from the Piracicaba River presented more aromatic moieties and fewer nitrogenous structures compared to the Tietê River. The presence of nitrogenous structures and fluorophores related to microbial activity can be an indicator of OM quality, which could be used as a global indicator of the river state. Thus, the combination of elemental and spectroscopic techniques allows for the successful deciphering of extracted OM characteristics. This approach can therefore be used as a tool to assess the quality of aquatic bodies.

Declaration of competing interest

The authors declare that they have no known competing financial interests or personal relationships that could have appeared to influence the work reported in this paper.

Acknowledgements

This study was partly financed by the Coordenação de Aperfeiçoamento de Pessoal de Nível Superior – Brasil (CAPES) Finance Code 001 grant number (88882.331025/2019-01) for the fellowship provided to Carla Pereira de Moraes, FAPESP grant number (2013/07276-1), and IHSS grant number (TRA 2019-9). The authors would like to thank Dr. R. Redon for providing support for PROGMEFF.

482 **References**

- 483 Bento, L.R., Constantino, I.C., Tadini, A.M., Melo, C.A., Ferreira, O.P., Moreira, A.B.,
484 Bisinoti, M.C., 2020. Chemical and Spectroscopic Characteristics of Anthrosol
485 (Amazonian Dark Earth) and Surrounding Soil from the Brazilian Amazon Forest:
486 Evaluation of Mineral and Organic Matter Content by Depth. *J. Braz. Chem. Soc.*
487 31, 1623–1634. <https://doi.org/10.21577/0103-5053.20200048>
- 488 Bernardo, N., Watanabe, F., Rodrigues, T., Alcântara, E., 2016. Evaluation of the
489 suitability of MODIS, OLCI and OLI for mapping the distribution of total
490 suspended matter in the Barra Bonita Reservoir (Tietê River, Brazil). *Remote Sens.*
491 *Appl. Soc. Environ.* 4, 68–82. <https://doi.org/10.1016/j.rsase.2016.06.002>
- 492 Bloesch, J., 2009. Sediments of Aquatic Ecosystems, in: Likens, G.E. (Ed.),
493 *Encyclopedia of Inland Waters*. Academic Press, Oxford, pp. 479–490.
494 <https://doi.org/10.1016/B978-012370626-3.00210-6>
- 495 Boguta, P., Sokołowska, Z., 2020. Zinc binding to fulvic acids: Assessing the impact of
496 pH, metal concentrations and chemical properties of fulvic acids on the mechanism
497 and stability of formed soluble complexes. *Molecules* 25, 1297.
498 <https://doi.org/10.3390/molecules25061297>
- 499 Boguta, P., Sokołowska, Z., 2016. Interactions of Zn(II) Ions with Humic Acids Isolated
500 from Various Type of Soils. Effect of pH, Zn Concentrations and Humic Acids
501 Chemical Properties. *PLoS One* 11, 1–20.
502 <https://doi.org/10.1371/journal.pone.0153626>
- 503 Borisover, M., Laor, Y., Parparov, A., Bukhanovsky, N., Lado, M., 2009. Spatial and
504 seasonal patterns of fluorescent organic matter in Lake Kinneret (Sea of Galilee)
505 and its catchment basin. *Water Res.* 43, 3104–3116.
506 <https://doi.org/10.1016/j.watres.2009.04.039>
- 507 Brailsford, F.L., Glanville, H.C., Golyshin, P.N., Johnes, P.J., Yates, C.A., Jones, D.L.,
508 2019. Microbial uptake kinetics of dissolved organic carbon (DOC) compound
509 groups from river water and sediments. *Sci. Rep.* 9, 11229.
510 <https://doi.org/10.1038/s41598-019-47749-6>
- 511 Brym, A., Paerl, H.W., Montgomery, M.T., Handsel, L.T., Ziervogel, K., Osburn, C.L.,
512 2014. Optical and chemical characterization of base-extracted particulate organic

- 513 matter in coastal marine environments. *Mar. Chem.* 162, 96–113.
 514 <https://doi.org/10.1016/j.marchem.2014.03.006>
- 515 Burdige, D.J., 2007. Preservation of organic matter in marine sediments: Controls,
 516 mechanisms, and an imbalance in sediment organic carbon budgets? *Chem. Rev.*
 517 107, 467–485. <https://doi.org/10.1021/cr050347q>
- 518 Burone, L., Muniz, P., Pires-vanin, A.N.A.M.S., 2003. Spatial distribution of organic
 519 matter in the surface sediments of Ubatuba Bay (Southeastern – Brazil) 75, 77–90.
 520 <https://doi.org/10.1590/S0001-37652003000100009>
- 521 Castillo, M.M., 2020. Suspended sediment, nutrients, and chlorophyll in tropical
 522 floodplain lakes with different patterns of hydrological connectivity. *Limnologica*
 523 82, 125767. <https://doi.org/10.1016/j.limno.2020.125767>
- 524 CETESB – Companhia de Tecnologia de Saneamento Ambiental, 2018. Relatório anual
 525 de Qualidade das Águas interiores no Estado de São Paulo 2017. <
 526 [https://cetesb.sp.gov.br/aguas-interiores/wp-content/uploads/sites/12/2018/06/Relat](https://cetesb.sp.gov.br/aguas-interiores/wp-content/uploads/sites/12/2018/06/Relat%C3%B3rio-de-Qualidade-das-%C3%81guas-Interiores-no-Estado-de-S%C3%A3o-Paulo-2017.pdf)
 527 [%C3%B3rio-de-Qualidade-das-%C3%81guas-Interiores-no-Estado-de-S](https://cetesb.sp.gov.br/aguas-interiores/wp-content/uploads/sites/12/2018/06/Relat%C3%B3rio-de-Qualidade-das-%C3%81guas-Interiores-no-Estado-de-S%C3%A3o-Paulo-2017.pdf)
 528 [%C3%A3o-Paulo-2017.pdf](https://cetesb.sp.gov.br/aguas-interiores/wp-content/uploads/sites/12/2018/06/Relat%C3%B3rio-de-Qualidade-das-%C3%81guas-Interiores-no-Estado-de-S%C3%A3o-Paulo-2017.pdf)>.
- 529 Chen, Z., Zhu, Z., Song, J., Liao, R., Wang, Y., Luo, X., Nie, D., Lei, Y., Shao, Y.,
 530 Yang, W., 2019. Linking biological toxicity and the spectral characteristics of
 531 contamination in seriously polluted urban rivers. *Environ. Sci. Eur.* 31, 1–10.
 532 <https://doi.org/10.1186/s12302-019-0269-y>
- 533 Coble, P.G., 1996. Characterization of marine and terrestrial DOM in seawater using
 534 excitation-emission matrix spectroscopy. *Mar. Chem.* 51, 325–346.
 535 [https://doi.org/10.1016/0304-4203\(95\)00062-3](https://doi.org/10.1016/0304-4203(95)00062-3)
- 536 Cole, J.J., Prairie, Y.T., Caraco, N.F., McDowell, W.H., Tranvik, L.J., Striegl, R.G.,
 537 Duarte, C.M., Kortelainen, P., Downing, J.A., Middelburg, J.J., Melack, J., 2007.
 538 Plumbing the global carbon cycle: Integrating inland waters into the terrestrial
 539 carbon budget. *Ecosystems* 10, 171–184. [https://doi.org/10.1007/s10021-006-](https://doi.org/10.1007/s10021-006-9013-8)
 540 [9013-8](https://doi.org/10.1007/s10021-006-9013-8)
- 541 Cruz, B.B., Manfré, L.A., Ricci, D.S., Brunoro, D., Appolinario, L., Quintanilha, J.A.,
 542 2017. Environmental fragility framework for water supply systems: a case study in
 543 the Paulista Macro Metropolis area (SE Brazil). *Environ. Earth Sci.* 76, 441.

544 <https://doi.org/10.1007/s12665-017-6778-3>

545 dos Santos, M.A., Rosa, L.P., Sikar, B., Sikar, E., dos Santos, E.O., 2006. Gross
546 greenhouse gas fluxes from hydro-power reservoir compared to thermo-power
547 plants. *Energy Policy* 34, 481–488. <https://doi.org/10.1016/j.enpol.2004.06.015>

548 Du, Y.X., Lu, Y.H., Roebuck, J.A., Liu, D., Chen, F.Z., Zeng, Q.F., Xiao, K., He, H.,
549 Liu, Z.W., Zhang, Y.L., Jaffé, R., 2021. Direct versus indirect effects of human
550 activities on dissolved organic matter in highly impacted lakes. *Sci. Total Environ.*
551 752, 141839. <https://doi.org/10.1016/j.scitotenv.2020.141839>

552 Duarte, C.M., 1995. Submerged aquatic vegetation in relation to different nutrient
553 regimes. *Ophelia* 41, 87–112. <https://doi.org/10.1080/00785236.1995.10422039>

554 Dungait, J.A.J., Hopkins, D.W., Gregory, A.S., Whitmore, A.P., 2012. Soil organic
555 matter turnover is governed by accessibility not recalcitrance. *Glob. Chang. Biol.*
556 18, 1781–1796. <https://doi.org/10.1111/j.1365-2486.2012.02665.x>

557 Edzwald, J.K., Tobiason, J.E., 2011. Water quality & treatment. A handbook on
558 drinking water, 6th ed. McGraw-Hill Professional Publishing, Colorado.

559 Engel, M.H., Macko, S.A., 2013. Organic Geochemistry: Principles and Applications.
560 Springer science & business media.

561 Funkey, C.P., Conley, D.J., Stedmon, C.A., 2019. Sediment alkaline-extracted organic
562 matter (AEOM)fluorescence: An archive of Holocene marine organic matter
563 origins. *Sci. Total Environ.* 676, 298–304.
564 <https://doi.org/10.1016/j.scitotenv.2019.04.170>

565 Guigue, J., Mathieu, O., Lévêque, J., Mounier, S., Laffont, R., Maron, P.A., Navarro,
566 N., Chateau, C., Amiotte-Suchet, P., Lucas, Y., 2014. A comparison of extraction
567 procedures for water-extractable organic matter in soils. *Eur. J. Soil Sci.* 65, 520–
568 530. <https://doi.org/10.1111/ejss.12156>

569 He, Z., Xu, S., Zhao, Y., Pan, X., 2019. Methane emissions from aqueous sediments are
570 influenced by complex interactions among microbes and environmental factors: A
571 modeling study. *Water Res.* 166, 115086.
572 <https://doi.org/10.1016/j.watres.2019.115086>

573 Henrichs, S.M., 1992. Early diagenesis of organic matter in marine sediments: progress

574 and perplexity. *Mar. Chem.* 39, 119–149. <https://doi.org/10.1016/0304->
575 4203(92)90098-U

576 Kaushal, S., Binford, M.W., 1999. Relationship between C:N ratios of lake sediments,
577 organic matter sources, and historical deforestation in Lake Pleasant,
578 Massachusetts, USA. *J. Paleolimnol.* 22, 439–442.
579 <https://doi.org/10.1023/A:1008027028029>

580 Kindler, R., Siemens, J., Kaiser, K., Walmsley, D.C., Bernhofer, C., Buchmann, N.,
581 Cellier, P., Eugster, W., Gleixner, G., Grunwald, T., Heim, A., Ibrom, A., Jones,
582 S.K., Jones, M., Klumpp, K., Kutsch, W., Larsen, K.S., Lehuger, S., Loubet, B.,
583 Mckenzie, R., Moors, E., Osborne, B., Pilegaard, K., Rebmann, C., Saunders, M.,
584 Schmidt, M.W.I., Schrumpf, M., Seyfferth, J., Skiba, U., Soussana, J.F., Sutton,
585 M.A., Tefs, C., Vowinkel, B., Zeeman, M.J., Kaupenjohann, M., 2011. Dissolved
586 carbon leaching from soil is a crucial component of the net ecosystem carbon
587 balance. *Glob. Chang. Biol.* 17, 1167–1185. <https://doi.org/10.1111/j.1365->
588 2486.2010.02282.x

589 Kleber, M., Lehmann, J., 2019. Humic Substances Extracted by Alkali Are Invalid
590 Proxies for the Dynamics and Functions of Organic Matter in Terrestrial and
591 Aquatic Ecosystems. *J. Environ. Qual.* 48, 207–216.
592 <https://doi.org/10.2134/jeq2019.01.0036>

593 Kothawala, D.N., Murphy, K.R., Stedmon, C.A., Weyhenmeyer, G.A., Tranvik, L.J.,
594 2013. Inner filter correction of dissolved organic matter fluorescence. *Limnol.*
595 *Oceanogr. Methods* 11, 616–630. <https://doi.org/10.4319/lom.2013.11.616>

596 Kowalczyk, P., Durako, M.J., Young, H., Kahn, A.E., Cooper, W.J., Gonsior, M., 2009.
597 Characterization of dissolved organic matter fluorescence in the South Atlantic
598 Bight with use of PARAFAC model: Interannual variability. *Mar. Chem.* 113,
599 182–196. <https://doi.org/10.1016/j.marchem.2009.01.015>

600 Kubo, A., Kanda, J., 2020. Coastal urbanization alters carbon cycling in Tokyo Bay.
601 *Sci. Rep.* 10, 1–11. <https://doi.org/10.1038/s41598-020-77385-4>

602 Kumwimba, M.N., Zhu, B., Suanon, F., Muyembe, D.K., Dzakpasu, M., 2017. Long-
603 term impact of primary domestic sewage on metal/lloid accumulation in drainage
604 ditch sediments, plants and water: Implications for phytoremediation and

605 restoration. *Sci. Total Environ.* 581–582, 773–781.
606 <https://doi.org/10.1016/j.scitotenv.2017.01.007>

607 Kurek, M.R., Harir, M., Shukle, J.T., Schroth, A.W., Schmitt-Kopplin, P., Druschel,
608 G.K., 2020. Chemical fractionation of organic matter and organic phosphorus
609 extractions from freshwater lake sediment. *Anal. Chim. Acta* 1130, 29–38.
610 <https://doi.org/10.1016/j.aca.2020.07.013>

611 Lawaetz, A.J., Stedmon, C.A., 2009. Fluorescence intensity calibration using the Raman
612 scatter peak of water. *Appl. Spectrosc.* 63, 936–940.
613 <https://doi.org/10.1366/000370209788964548>

614 Lehmann, J., Hansel, C.M., Kaiser, C., Kleber, M., Maher, K., Manzoni, S., Nunan, N.,
615 Reichstein, M., Schimel, J.P., Torn, M.S., Wieder, W.R., Kögel-Knabner, I., 2020.
616 Persistence of soil organic carbon caused by functional complexity. *Nat. Geosci.*
617 13, 529–534. <https://doi.org/10.1038/s41561-020-0612-3>

618 Meyers, P.A., 1994. Preservation of elemental and isotopic source identification of
619 sedimentary organic matter. *Chem. Geol.* 114, 289–302.
620 [https://doi.org/10.1016/0009-2541\(94\)90059-0](https://doi.org/10.1016/0009-2541(94)90059-0)

621 Morais, C.P., Nicolodelli, G., Mitsuyuki, M.C., Silva, K.S.G., Mauad, F.F., Mounier, S.,
622 Milori, D.M.B.P., 2021. Total phosphorus determination in eutrophic tropical river
623 sediments by laser-induced breakdown spectroscopy techniques. *Anal. Methods*
624 13, 77–83. <https://doi.org/10.1039/d0ay02008g>

625 Mounier, S., Zhao, H., Garnier, C., Redon, R., 2011. Copper complexing properties of
626 dissolved organic matter: PARAFAC treatment of fluorescence quenching.
627 *Biogeochemistry* 106, 107–116. <https://doi.org/10.1007/s10533-010-9486-6>

628 Muller, M., Jimenez, J., Antonini, M., Dudal, Y., Latrille, E., Vedrenne, F., Steyer, J.P.,
629 Patureau, D., 2014. Combining chemical sequential extractions with 3D
630 fluorescence spectroscopy to characterize sludge organic matter. *Waste Manag.* 34,
631 2572–2580. <https://doi.org/10.1016/j.wasman.2014.07.028>

632 Murdoch, A., MacKnight, S. (Eds.), 1991. *Handbook of Techniques for Aquatic*
633 *Sediments Sampling*. CRC Press, Boca Raton.

634 Murphy, K.R., Stedmon, C.A., Wenig, P., Bro, R., 2014. OpenFluor- An online spectral

635 library of auto-fluorescence by organic compounds in the environment. *Anal.*
 636 *Methods* 6, 658–661. <https://doi.org/10.1039/c3ay41935e>

637 Nixon, S.W., 1995. Coastal marine eutrophication: A definition, social causes, and
 638 future concerns. *Ophelia* 41, 199–219.
 639 <https://doi.org/10.1080/00785236.1995.10422044>

640 Olk, D.C., Bloom, P.R., Perdue, E.M., McKnight, D.M., Chen, Y., Farenhorst, A.,
 641 Senesi, N., Chin, Y.-P., Schmitt-Kopplin, P., Hertkorn, N., Harir, M., 2019.
 642 Environmental and Agricultural Relevance of Humic Fractions Extracted by Alkali
 643 from Soils and Natural Waters. *J. Environ. Qual.* 48, 217–232.
 644 <https://doi.org/10.2134/jeq2019.02.0041>

645 Osburn, C.L., Boyd, T.J., Montgomery, M.T., Bianchi, T.S., Coffin, R.B., Paerl, H.W.,
 646 2016. Optical proxies for terrestrial dissolved organic matter in estuaries and
 647 coastal waters. *Front. Mar. Sci.* 2, 127. <https://doi.org/10.3389/fmars.2015.00127>

648 Osburn, C.L., Wigdahl, C.R., Fritz, S.C., Saros, J.E., 2011. Dissolved organic matter
 649 composition and photoreactivity in prairie lakes of the U.S. Great Plains. *Limnol.*
 650 *Oceanogr.* 56, 2371–2390. <https://doi.org/10.4319/lo.2011.56.6.2371>

651 Redon, R., Mounier, S., 2018. PROGMEEF. < <https://woms18.univ-tln.fr/progmeef/>>.

652 Rocha, P.S., Azab, E., Schmidt, B., Storch, V., Hollert, H., Braunbeck, T., 2010.
 653 Changes in toxicity and dioxin-like activity of sediments from the Tietê River (São
 654 Paulo, Brazil). *Ecotoxicol. Environ. Saf.* 73, 550–558.
 655 <https://doi.org/10.1016/j.ecoenv.2009.12.017>

656 Rocha, P.S., Bernecker, C., Strecker, R., Mariani, C.F., Pompô, M.L.M., Storch, V.,
 657 Hollert, H., Braunbeck, T., 2011. Sediment-contact fish embryo toxicity assay with
 658 *Danio rerio* to assess particle-bound pollutants in the Tietê River Basin (São Paulo,
 659 Brazil). *Ecotoxicol. Environ. Saf.* 74, 1951–1959.
 660 <https://doi.org/10.1016/j.ecoenv.2011.07.009>

661 Rodrigues, T., Alcântara, E., Rotta, L., Bernardo, N., Watanabe, F., 2020. An
 662 investigation into the relationship between light absorption budget and trophic
 663 status in inland waters. *Ecol. Indic.* 115, 106410.
 664 <https://doi.org/10.1016/j.ecolind.2020.106410>

- 665 Schorer, M., Eisele, M., 1997. Accumulation of inorganic and organic pollutants by
666 biofilms in the aquatic environment. *Water, Air Soil Pollut.* 99, 651–659.
- 667 Shutova, Y., Baker, A., Bridgeman, J., Henderson, R.K., 2014. Spectroscopic
668 characterisation of dissolved organic matter changes in drinking water treatment:
669 From PARAFAC analysis to online monitoring wavelengths. *Water Res.* 54, 159–
670 169. <https://doi.org/10.1016/j.watres.2014.01.053>
- 671 Sire, J., Klavins, M., Kreismanis, J., Jansone, S., 2009. Impact of the process of
672 isolating humic acids from peat on their properties. *Can. J. Civ. Eng.* 36, 345–355.
673 <https://doi.org/10.1139/S08-052>
- 674 Smith, W.S., Espíndola, E.L.G., Rocha, O., 2014. Environmental gradient in reservoirs
675 of the medium and low Tietê River: limnological differences through the habitat
676 sequence. *Acta Limnol. Bras.* 26, 73–88. [https://doi.org/10.1590/s2179-](https://doi.org/10.1590/s2179-975x2014000100009)
677 [975x2014000100009](https://doi.org/10.1590/s2179-975x2014000100009)
- 678 Soares da Silva, L., Constantino, I.C., Bento, L.R., Tadini, A.M., Bisinoti, M.C.,
679 Boscolo, M., Ferreira, O.P., Mounier, S., Piccolo, A., Spaccini, R., Cornélio, M.L.,
680 Moreira, A.B., 2020. Humic extracts from hydrochar and Amazonian Anthrosol:
681 Molecular features and metal binding properties using EEM-PARAFAC and 2D
682 FTIR correlation analyses. *Chemosphere* 256, 1–12.
683 <https://doi.org/10.1016/j.chemosphere.2020.127110>
- 684 Veres, D.S., 2002. A comparative study between loss on ignition and total carbon
685 analysis on mineralogenic sediments. *Stud. UBB Geol.* 47, 171–182.
686 <http://dx.doi.org/10.5038/1937-8602.47.1.13>
- 687 Walker, S.A., Amon, R.M.W., Stedmon, C.A., 2013. Variations in high-latitude riverine
688 fluorescent dissolved organic matter: A comparison of large Arctic rivers. *J.*
689 *Geophys. Res. Biogeosciences* 118, 1689–1702.
690 <https://doi.org/10.1002/2013JG002320>
- 691 Weishaar, J.L., Fram, M.S., Fujii, R., Mopper, K., 2003. Evaluation of Specific
692 Ultraviolet Absorbance as an Indicator of the Chemical Composition and
693 Reactivity of Dissolved Organic Carbon. *Environ. Sci. Technol.* 37, 4702–4708.
694 <https://doi.org/10.1021/es030360x>
- 695 Yamashita, Y., Cory, R.M., Nishioka, J., Kuma, K., Tanoue, E., Jaffé, R., 2010a.

696 Fluorescence characteristics of dissolved organic matter in the deep waters of the
 697 Okhotsk Sea and the northwestern North Pacific Ocean. *Deep. Res. Part II Top.*
 698 *Stud. Oceanogr.* 57, 1478–1485. <https://doi.org/10.1016/j.dsr2.2010.02.016>

699 Yamashita, Y., Jaffé, R., Maie, N., Tanoue, E., 2008. Assessing the dynamics of
 700 dissolved organic matter (DOM) in coastal environments by excitation emission
 701 matrix fluorescence and parallel factor analysis (EEM-PARAFAC). *Limnol.*
 702 *Oceanogr.* 53, 1900–1908. <https://doi.org/10.4319/lo.2008.53.5.1900>

703 Yamashita, Y., Scinto, L.J., Maie, N., Jaffé, R., 2010b. Dissolved Organic Matter
 704 Characteristics Across a Subtropical Wetland's Landscape: Application of Optical
 705 Properties in the Assessment of Environmental Dynamics. *Ecosystems* 13, 1006–
 706 1019. <https://doi.org/10.1007/s10021-010-9370-1>

707 Zepp, R.G., Sheldon, W.M., Moran, M.A., 2004. Dissolved organic fluorophores in
 708 southeastern US coastal waters: Correction method for eliminating Rayleigh and
 709 Raman scattering peaks in excitation-emission matrices. *Mar. Chem.* 89, 15–36.
 710 <https://doi.org/10.1016/j.marchem.2004.02.006>

711 Zhang, L., Liu, H., Peng, Y., Zhang, Y., Sun, Q., 2020. Characteristics and significance
 712 of dissolved organic matter in river sediments of extremely water-deficient basins:
 713 A Beiyun River case study. *J. Clean. Prod.* 277, 123063.
 714 <https://doi.org/10.1016/j.jclepro.2020.123063>

715